

# Testing physical models for dipolar asymmetry: from temperature to $k$ space to lensing

J. P. Zibin<sup>1,\*</sup> and D. Contreras<sup>1,†</sup>

<sup>1</sup>*Department of Physics & Astronomy  
University of British Columbia, Vancouver, BC, V6T 1Z1 Canada*

(Dated: April 5, 2024)

One of the most intriguing hints of a departure from the standard cosmological model is a large-scale dipolar power asymmetry in the cosmic microwave background (CMB). If not a statistical fluke, its origins must lie in the modulation of the position-space fluctuations via a physical mechanism, which requires the observation of new modes to confirm or refute. We introduce an approach to describe such a modulation in  $k$  space and calculate its effects on the CMB temperature and lensing. We fit the  $k$ -space modulation parameters to *Planck* 2015 temperature data and show that CMB lensing will not provide us with enough independent information to confirm or refute such a mechanism. However, our approach elucidates some poorly understood aspects of the asymmetry, in particular that it is weakly constrained. Also, it will be particularly useful in predicting the effectiveness of polarization in testing a physical modulation.

PACS numbers: 98.70.Vc, 98.80.Es, 98.80.Jk

## I. INTRODUCTION

The standard cosmological model, known as  $\Lambda$  cold dark matter ( $\Lambda$ CDM), describes the large-scale and early Universe remarkably well, with only a handful of parameters (see, e.g., [1]). Very few hints of departures or tensions with  $\Lambda$ CDM exist in the present cosmological data. Of these, considerable attention has been paid to various so-called “anomalies” in measurements of the cosmic microwave background (CMB) radiation (see, e.g., [2–4]). In some cases, the anomalies are known to become statistically insignificant when correcting for the line-of-sight integrated Sachs-Wolfe (ISW) contribution (see, e.g., [5–7]). In these cases, due to the weak correlation between the ISW and primary anisotropies, the anomalies are unlikely to be due to some physical mechanism and hence are almost certainly statistical flukes. However, in all cases the anomalies are of only weak to moderate statistical significance, which typically is reduced further when correcting for *a posteriori* selection effects (also known as the “look elsewhere effect”) [2, 3].

One intriguing feature of the CMB temperature ( $T$ ) anisotropies is a roughly dipolar power asymmetry [8]. Measurements with the *Planck* mission [3] indicate a roughly 6% amplitude of asymmetry up to multipole  $\ell \simeq 65$ , with a significance (as measured by a  $p$  value) of roughly 1%. Equivalently, the measured amplitude is only about 2–2.5 times the expected level of asymmetry due to cosmic variance in statistically isotropic skies [3]. The significance of the asymmetry becomes lower out to higher  $\ell$  [3, 9–11], and is reduced to of order 10% if we do not consider the scale  $\ell \simeq 65$  as predicted and correct for *a posteriori* effects [2, 3].

However, despite its underwhelming statistical signif-

icance the dipolar power asymmetry remains interesting because of its large-scale character. The asymmetry involves scales that are roughly super-Hubble at last scattering, and a number of early-Universe or inflationary mechanisms might conceivably affect these scales preferentially. For example, CDM isocurvature fluctuations naturally imprint on scales  $\ell \lesssim 100$ . However, a particular modulated isocurvature model [12] was recently tested [13] and found to not be preferred to  $\Lambda$ CDM.

More generally, it appears to be very difficult to construct a physical mechanism for generating a scale-dependent dipolar modulation (see [14] for a thorough discussion and summary of previous attempts). This contrasts with the relative ease in producing a *quadrupolar* modulation (see, e.g., [15–17]). The crucial difference is that a quadrupolar asymmetry on the sky can be produced via a quadrupolar statistical anisotropy in  $k$  space, associated, e.g., with a homogeneous vector field. However, despite some claims to the contrary [18], a  $k$ -space anisotropy cannot lead to a dipolar asymmetry on the sky: the reality of the fluctuations implies that the  $k$ -space power spectrum must have even parity (see, e.g., [19]). Instead, a dipolar asymmetry must be the result of statistical *inhomogeneity*, perhaps due to modulation with a long-wavelength mode. Note that this distinction holds more generally for any odd compared with any even type of asymmetry. (Parity violation may circumvent this argument; see, e.g., [20].)

It is clear that the important question of whether the observed dipolar asymmetry in the CMB temperature fluctuations is due to a statistical fluke or to a real, physical modulation of the primordial fluctuations will not be resolved through further study of the temperature fluctuations. This is simply because the large-scale  $T$  data are already cosmic-variance limited, so there will be no significant reduction of noise by remeasuring them. What are needed are observations that can probe *independent* fluctuation modes from those which source temperature. The most obvious such observations are of the CMB po-

\*Electronic address: [zibin@phas.ubc.ca](mailto:zibin@phas.ubc.ca)

†Electronic address: [dagocont@phas.ubc.ca](mailto:dagocont@phas.ubc.ca)

larization. Although  $E$ -mode polarization is partially correlated with temperature, it is largely sourced by independent modes. Polarization has long been recognized as useful for providing independent checks of “anomalies” found in the  $T$  data (see, e.g., [21–24]).

It is worthwhile considering whether observations other than polarization might also be able to address this question. The essential difficulty is that the scales at which the  $T$  asymmetry is observed are extremely large. To illustrate this, we plot in Fig. 1 the Limber approximation kernels for various cosmological observations in the  $k$ - $r$  plane. (See [25] for details on the calculations involved.) The vertical line indicates the  $k$  scale corresponding approximately to multipole  $\ell = 65$  in the primary CMB. We can see that only the ISW effect and CMB lensing are currently capable of reaching the required large scales. (Nevertheless, limits on dipolar asymmetry in the quasar distribution on much smaller scales were placed in [26].) However, the ISW effect is mainly sourced at low redshifts. Therefore, for a primordial fluctuation modulation *linear* in position, the modulation amplitude would be expected to be very small for the ISW effect (we will see this explicitly for the case of lensing in Sec. IV). In addition the ISW contribution mainly appears at the very smallest multipoles, so will be heavily affected by cosmic variance.

Therefore it appears that, after polarization, CMB lensing offers the best chance at testing the asymmetry. However, it should be apparent from Fig. 1 that, as with the ISW effect, lensing is sourced considerably closer to us than the primary CMB, and hence, for a spatially linear modulation, we expect a lower modulation amplitude. In addition, the  $k$  scales modulated in the CMB will appear at larger angular scales, i.e. we expect the asymmetry to appear to lower maximum multipole, in lensing. Thus we expect fewer modulated modes for lensing than for temperature. For these reasons we expect the significance of detection achievable with lensing to be lower than that from temperature. On the other hand, the modes sourcing lensing will be essentially completely uncorrelated with the primary CMB temperature, whereas CMB polarization shares significant correlation with temperature.

While most previous studies of the CMB large-scale asymmetry have been restricted to  $\ell$  or map space, if we observe some amplitude of asymmetry out to some multipole scale in temperature we do not expect a CMB lensing modulation of the same amplitude and scales, as just explained. This same point will also apply to polarization, due to the different kernels from  $k$  space to multipole space for these observations. Therefore, in order to obtain predictions for lensing or polarization we must proceed via a  $k$ -space (or position-space) modulation model.

In this paper we have two main goals. The first is to present a formalism for fitting a  $k$ -space modulation to CMB  $T$  data. This involves first describing a spatially linear modulation in  $k$  space, and then deriving its effect on the  $T$  fluctuations. We show that this effect can be

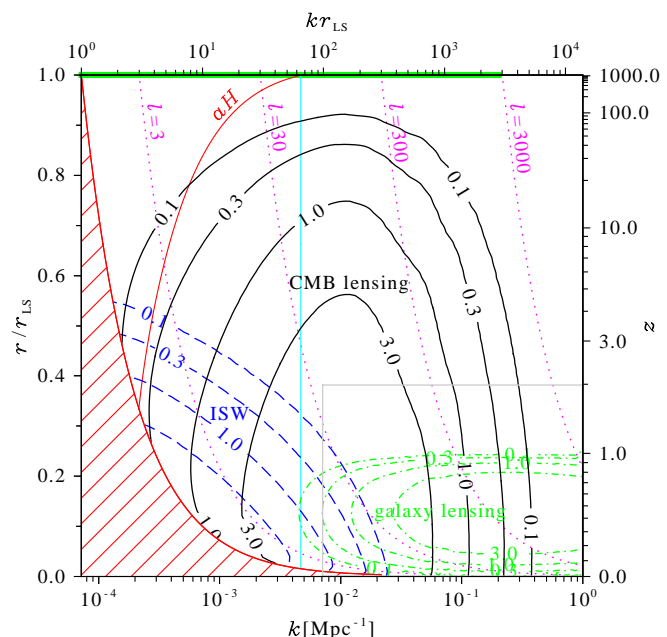


FIG. 1: Limber approximation kernels (in arbitrary units) for various cosmological observations (contours) out to last scattering ( $r = r_{\text{LS}}$ ). The grey box indicates very roughly the reach of the planned Euclid survey [27]. Dotted magenta curves correspond to fixed multipole scales, with the red hatched region geometrically inaccessible. The vertical cyan line corresponds approximately to the scale  $\ell = 65$  in the primary CMB (narrow green box at the top); scales roughly to the left of it exhibit dipolar asymmetry in the CMB. To test a modulation model, many more modes are available in principle in our observable volume than in the primary CMB source region. Adapted from [25].

calculated accurately in a very simple way. We then fit the modulation to *Planck*  $T$  data using Bayesian parameter estimation. Our next goal is to determine what the  $k$ -space model predicts for CMB lensing. To do this we must introduce a formalism for calculating the effect of a  $k$ -space modulation on lensing.

Our approach will also be applicable to predicting the signal of modulation in CMB polarization based on the  $T$  observations. However, besides providing such predictions, our rigorous approach to fitting is important in its own right. While grounding the study of the asymmetry firmly in  $k$  space, we find that temperature data alone are not constraining enough to clearly define a  $k$ -space modulation. In particular, the often-quoted 6% modulation out to  $\ell \simeq 65$  does not stand out in the data.

In previous related work, [28] predicted the polarization asymmetry given a simplified procedure for fitting to the  $T$  data, for modulations of various cosmological parameters. Reference [29] considered what the  $T$  asymmetry predicts for polarization asymmetry via modulated primordial spectra, using a similar fitting procedure. Importantly, they found that the polarization predictions are strongly dependent on the  $k$ -space model. Refs. [30, 31] performed more careful fitting, but restricted their models. None of these groups considered

lensing. Ref. [9] looked for a power asymmetry in the *Planck* lensing map, finding no significant signal in the low- $\ell$   $T$  asymmetry direction. Additionally, a recent study [32] claimed that lensing  $B$  modes could confirm a physical modulation at high significance, due to the mode mixing that takes low- $\ell$  lensing modes to high- $\ell$   $B$  modes. However, this paper treated the statistics of the lensed  $B$  field as Gaussian, whereas it is known that non-Gaussianity reduces the total signal-to-noise ratio of the lensing  $B$  power spectrum by a large factor (see, e.g., [33]). Also, [32] did not consider a physical lensing modulation mechanism and simply took the expected lensing modulation amplitude to be 7% to  $\ell = 70$ .

In this paper we approach this topic in a much more rigorous way. In the first few sections we lay out our modulation formalism. Section II describes our treatment of the  $k$ -space modulation, while Secs. III and IV derive the effects of the  $k$ -space modulation on CMB temperature anisotropies and the lensing potential, respectively. The following sections present our approach to fitting the  $k$ -space modulation to the CMB temperature data (Sec. V), and describe the predicted effect of the modulation on the CMB lensing (Sec. VI).

Throughout this paper we use the set of  $\Lambda$ CDM cosmological parameters chosen for the Planck Collaboration Full Focal Plane (FFP8) simulations; namely, we set Hubble parameter  $H_0 = 100 h \text{ km s}^{-1} \text{ Mpc}^{-1}$ , with  $h = 0.6712$ , baryon density  $\Omega_b h^2 = 0.0222$ , CDM density  $\Omega_c h^2 = 0.1203$ , neutrino density  $\Omega_\nu h^2 = 0.00064$ , cosmological constant density parameter  $\Omega_\Lambda = 0.6823$ , primordial comoving curvature perturbation power spectrum amplitude  $A_s = 2.09 \times 10^{-9}$  at pivot scale  $k_0 = 0.05 \text{ Mpc}^{-1}$  and tilt  $n_s = 0.96$ , and optical depth to reionization  $\tau = 0.065$ . However, we expect our results to be only very weakly dependent on these parameters.

## II. PRIMORDIAL ADIABATIC $k$ -SPACE MODULATION

Our basic premise is to ask: *If* the large-scale CMB temperature dipolar asymmetry is due to a real, physical modulation of the primordial fluctuations, then what would this predict for CMB lensing (or polarization)? As discussed in the Introduction, a  $T$  asymmetry of, say, 6% to  $\ell \simeq 65$  will not correspond to a lensing (or polarization) modulation of the same amplitude and angular scales. To proceed we must specify a form for a primordial modulation in position or  $k$  space. This could take the form of a modulation of the large-scale adiabatic fluctuations, or alternatively a CDM isocurvature or tensor modulation. The latter two are motivated by the fact that they naturally give a contribution only on large scales. Tensor modes, however, are expected to produce only tiny gradient-type lensing [34]. CDM isocurvature modes produce considerably less lensing than adiabatic modes, for comparable large-scale CMB  $T$  contributions. Therefore, we will restrict our analysis here to the modulation of adiabatic modes. However, when considering

the predictions for polarization, it will be important to consider these other fluctuation types as well [29].

It is clear that there is no significant *scale-independent* dipolar asymmetry in the CMB temperature fluctuations (see, e.g., [3]). Studies indicate an asymmetry amplitude of roughly 6% out to multipoles  $\ell \simeq 65$ , with decreasing amplitude to larger  $\ell$  [3]. This apparent scale dependence motivates us to treat the primordial adiabatic fluctuations as the sum of a large-scale dipole-modulated part and a small-scale statistically isotropic part. The scale dependence of the large-scale part will be free, although the total statistically isotropic power will agree with  $\Lambda$ CDM. In the following we will indicate modulated fields by a tilde, while statistically isotropic fields will have no tilde. We therefore write the total primordial (and hence time-independent) comoving curvature perturbation,  $\tilde{\mathcal{R}}(\mathbf{x})$ , as

$$\tilde{\mathcal{R}}(\mathbf{x}) = \tilde{\mathcal{R}}^{\text{lo}}(\mathbf{x}) + \mathcal{R}^{\text{hi}}(\mathbf{x}), \quad (1)$$

where the high- $k$  part is statistically isotropic,

$$\langle \mathcal{R}^{\text{hi}}(\mathbf{k}) \mathcal{R}^{\text{hi}*}(\mathbf{k}') \rangle = \frac{2\pi^2}{k^3} \mathcal{P}_{\mathcal{R}}^{\text{hi}}(k) \delta^3(\mathbf{k} - \mathbf{k}'). \quad (2)$$

On the other hand, the low- $k$  part is taken to be linearly modulated:

$$\tilde{\mathcal{R}}^{\text{lo}}(\mathbf{x}) = \mathcal{R}^{\text{lo}}(\mathbf{x}) \left( 1 + A_{\mathcal{R}} \frac{r}{r_{\text{LS}}} \cos \theta \right) \quad (3)$$

$$= \mathcal{R}^{\text{lo}}(\mathbf{x}) \left( 1 + A_{\mathcal{R}} \frac{z}{r_{\text{LS}}} \right), \quad (4)$$

where  $r_{\text{LS}}$  is the comoving radius to last scattering,  $A_{\mathcal{R}}$  is a constant, the “modulation amplitude”, and  $\theta$  is the angle from the modulation direction, which we here define to coincide with the  $\hat{z}$  direction.  $\mathcal{R}^{\text{lo}}$  satisfies

$$\langle \mathcal{R}^{\text{lo}}(\mathbf{k}) \mathcal{R}^{\text{lo}*}(\mathbf{k}') \rangle = \frac{2\pi^2}{k^3} \mathcal{P}_{\mathcal{R}}^{\text{lo}}(k) \delta^3(\mathbf{k} - \mathbf{k}'). \quad (5)$$

Finally, we take  $\mathcal{R}^{\text{lo}}$  and  $\mathcal{R}^{\text{hi}}$  to be uncorrelated,

$$\langle \mathcal{R}^{\text{lo}}(\mathbf{k}) \mathcal{R}^{\text{hi}*}(\mathbf{k}') \rangle = 0, \quad (6)$$

so that the total statistically isotropic fluctuations,  $\mathcal{R}(\mathbf{k}) \equiv \mathcal{R}^{\text{lo}}(\mathbf{k}) + \mathcal{R}^{\text{hi}}(\mathbf{k})$ , must have the usual  $\Lambda$ CDM power spectrum,

$$\langle \mathcal{R}(\mathbf{k}) \mathcal{R}^*(\mathbf{k}') \rangle = \frac{2\pi^2}{k^3} \mathcal{P}_{\mathcal{R}}^{\Lambda\text{CDM}}(k) \delta^3(\mathbf{k} - \mathbf{k}'), \quad (7)$$

where

$$\mathcal{P}_{\mathcal{R}}^{\Lambda\text{CDM}}(k) = \mathcal{P}_{\mathcal{R}}^{\text{lo}}(k) + \mathcal{P}_{\mathcal{R}}^{\text{hi}}(k). \quad (8)$$

In words, the full-sky “average” (or “equatorial”) power spectrum will agree with that of  $\Lambda$ CDM (at least to lowest order in  $A_{\mathcal{R}}$ ). As we explain below, treating the fields as two uncorrelated components does not restrict the generality of our approach.

Also, note that we have in mind that  $\mathcal{R}^{\text{hi}}$  contributes only negligibly to the largest scales, so that we expect  $A_{\mathcal{R}} \simeq 0.06$  when  $\mathcal{P}_{\mathcal{R}}^{\text{lo}}(k)$  extends only to scales corresponding to  $\ell \simeq 65$ , according to the observed  $T$  asymmetry. In this study we will take the low- $k$  modulated component to have the spectrum

$$\mathcal{P}_{\mathcal{R}}^{\text{lo}}(k) = \frac{1}{2}A_s \left(\frac{k}{k_0}\right)^{n_s-1} \left[1 - \tanh\left(\frac{\ln k - \ln k_c}{\Delta \ln k}\right)\right]. \quad (9)$$

This spectrum approaches the standard  $\Lambda$ CDM spectrum for small  $k$  and approaches zero for large  $k$ , with cutoff scale  $k_c$  and width of cutoff  $\Delta \ln k$ . Recall that the total (isotropic) power spectrum is still constrained to have the standard power-law form via Eq. (8). This particular tanh scale dependence is not intended to model any particular mechanism for the modulation of fluctuations. But it can capture some interesting cases. For large  $k_c$ , the modulation becomes scale-invariant. By decreasing  $k_c$  we can represent a modulation only on large scales, e.g. scales that are super-Hubble at last scattering, which may be related to some early-Universe process. For  $k_c \simeq 5 \times 10^{-3} \text{ Mpc}^{-1}$  and  $\Delta \ln k \rightarrow 0$  in particular, we produce a modulation on the commonly quoted angular scales of  $\ell \lesssim 65$  (keeping in mind that the  $k$ - $\ell$  kernels imply that there is no one-to-one correspondence between  $k$  and  $\ell$  values).

The form of the modulation in Eq. (4), i.e. that of a spatially linearly modulated primordial field, is an important assumption here. We regard it as the simplest form that would lead to a dipolar asymmetry. A linear modulation can be considered the lowest-order term in an expansion, for general modulations varying slowly on our Hubble scale. Other choices add complexity and require more parameters to specify, e.g., generalizing the linear form to quadratic or higher order spatial dependence, or taking the fluctuation spectrum to jump like a step function across a “wall”. These more complicated scenarios could be tested, since they would predict asymmetry beyond dipolar, but considering the low signal-to-noise ratio of the  $T$  asymmetry we restrict this study to the simplest possibility. Crucially, the linear modulation means that CMB lensing, which is mainly sourced at low redshifts, is expected to be modulated with considerably lower amplitude than the observed  $T$  amplitude of roughly 6%. This conclusion will clearly be strongly dependent on the assumed form of the  $k$ -space modulation. Also, note that we take the linear modulation to act on the *primordial* field,  $\mathcal{R}$ . This is what would be expected in most proposed models where the modulation originates in some very early physics, e.g. during inflation. Also, it leads to the linear dependence on *comoving* distance in Eq. (4). Conversely, it seems very unlikely that a late-time field (e.g. the zero-shear gauge fluctuation  $\psi_\sigma$ ; see below) would be directly modulated. Such a scenario could involve an anisotropic dark energy, which would be subject to strong constraints at the background level. Nevertheless, we will show that, insofar as CMB  $T$  and lensing are concerned, to a good approximation we can equally consider either the early- or late-time fields

to be linearly modulated.

In  $k$  space the modulation of Eq. (4) becomes

$$\tilde{\mathcal{R}}^{\text{lo}}(\mathbf{k}) = \mathcal{R}^{\text{lo}}(\mathbf{k}) + i \frac{A_{\mathcal{R}}}{r_{\text{LS}}} \frac{\partial}{\partial k_z} \mathcal{R}^{\text{lo}}(\mathbf{k}). \quad (10)$$

This implies that the total  $\tilde{\mathcal{R}}(\mathbf{k})$  covariance (to first order in  $A_{\mathcal{R}}$ ) is given by

$$\begin{aligned} \langle \tilde{\mathcal{R}}(\mathbf{k}) \tilde{\mathcal{R}}^*(\mathbf{k}') \rangle &= \frac{2\pi^2}{k^3} \mathcal{P}_{\mathcal{R}}^{\Lambda\text{CDM}}(k) \delta^3(\mathbf{k} - \mathbf{k}') \\ &\quad + 2\pi^2 i \frac{A_{\mathcal{R}}}{r_{\text{LS}}} \left[ \frac{\mathcal{P}_{\mathcal{R}}^{\text{lo}}(k)}{k^3} + \frac{\mathcal{P}_{\mathcal{R}}^{\text{lo}}(k')}{k'^3} \right] \\ &\quad \times \delta^2(\mathbf{k}_\perp - \mathbf{k}'_\perp) \delta'(k_z - k'_z), \end{aligned} \quad (11)$$

where  $\mathbf{k}_\perp$  is the projection of  $\mathbf{k}$  orthogonal to  $\hat{z}$  and the prime on the Dirac delta denotes a derivative with respect to the argument. Note importantly that, for a Gaussian field  $\tilde{\mathcal{R}}$ , Eq. (11) is a complete statistical description. This means that the details of our implementation, i.e. in terms of the components  $\mathcal{R}^{\text{lo}}$  and  $\mathcal{R}^{\text{hi}}$ , are irrelevant: in the end we obtain a covariance corresponding to a standard isotropic part (the diagonal part of Eq. (11)), plus a dipole-modulated part with arbitrary scale dependence, as determined by  $\mathcal{P}_{\mathcal{R}}^{\text{lo}}(k)$  (the off-diagonal, imaginary part of Eq. (11)). In particular, our approach does not restrict us to some early-Universe mechanism which produces two uncorrelated components,  $\mathcal{R}^{\text{lo}}$  and  $\mathcal{R}^{\text{hi}}$ . The separation into those two components is purely a convenient calculational device which will make the analytical work considerably simpler, as we will see next. We remain agnostic as to the physical modulation mechanism. Note that Eq. (11) describes *statistically inhomogeneous* fluctuations, whereas the effect in  $\ell$  or map space will be *statistical anisotropy*.

### III. EFFECT ON CMB TEMPERATURE ANISOTROPIES

#### A. Multipole covariance

In general, the effect of the modulation, Eq. (4), on the CMB anisotropies would be very difficult to calculate (see [31] for such a general approach). However, we will show that, to a very good approximation, the effect will be simply to introduce an  $\ell$  to  $\ell \pm 1$  coupling with spectrum determined by  $\mathcal{P}_{\mathcal{R}}^{\text{lo}}(k)$ , as one might intuitively expect for scales much smaller than the length scale of variation of the modulation.

We begin by demonstrating this on the largest scales, for which we can analytically write down the  $T$  anisotropies. Since the observed modulation is on large scales, this is a relevant regime. The large-scale approximation used here will begin to break down on scales  $\ell \sim 50$ , although in this case a simple argument will allow us to write down the multipole covariance immediately. Nevertheless, we will provide a detailed examination of the small-scale case in the [Appendix](#).



On the largest scales, it is a good approximation to treat the plasma as tightly coupled prior to an instantaneous recombination. In this approximation, the  $T$  anisotropies are determined entirely by the zero-shear (longitudinal) gauge metric perturbation,  $\psi_\sigma$ , which is related to the primordial comoving curvature perturbation,  $\mathcal{R}$ , via

$$\psi_\sigma(\mathbf{k}) = -\frac{3}{5}T(k)\mathcal{R}(\mathbf{k}), \quad (12)$$

where  $T(k)$  is the transfer function that captures the effect of radiation domination (see, e.g., [35]). Since here we are considering only the largest scales, we will ignore the component  $\mathcal{R}^{\text{hi}}$  in this subsection and drop the superscript “lo” for brevity.

Note that in general a linear modulation of  $\mathcal{R}$  will not imply a linear modulation of  $\psi_\sigma$ , i.e. the operations of linear modulation and filtering via  $T(k)$  will not commute. An easy way to see this is to consider the extreme case of a very narrow filtering around some scale  $\bar{k}$ ,  $T(k) \simeq \delta(k - \bar{k})$ . Then applying  $T(k)$  to the linearly modulated  $\mathcal{R}$  will simply give a nearly monospatial-frequency  $\psi_\sigma$ , which will not be spatially modulated, as opposed to the case of modulating the field filtered with  $T(k)$ . Therefore, in general, a linear primordial modulation does not lead to a corresponding linear modulation of  $\psi_\sigma$ , which is the field that determines the  $T$  anisotropies. In practice, this will mean that the calculation of the  $T$  anisotropies will be very difficult. On the other hand, for constant  $T(k)$ , the operations of modulation and filtering clearly commute. So as long as  $T(k)$  is sufficiently slowly varying, we will be able to assume commutativity to good approximation.

To determine the quantitative effect of the non-commutativity, Eq. (10) implies

$$T(k)\tilde{\mathcal{R}}(\mathbf{k}) = \left[ T(k) - i\frac{A_{\mathcal{R}}}{r_{\text{LS}}} \frac{k_z}{k} T'(k) \right] \mathcal{R}(\mathbf{k}) + i\frac{A_{\mathcal{R}}}{r_{\text{LS}}} \frac{\partial}{\partial k_z} [T(k)\mathcal{R}(\mathbf{k})]. \quad (13)$$

Comparing with Eq. (12), this tells us that if

$$\left| i\frac{1}{r_{\text{LS}}} \frac{k_z}{k} T'(k) \right| \ll T(k), \quad (14)$$

i.e., if

$$\left| \frac{1}{T(k)} \frac{dT(k)}{dkr_{\text{LS}}} \right| \ll 1, \quad (15)$$

then the operations of modulation and filtering will essentially commute, so that we can write the total  $\psi_\sigma$  fluctuations to a good approximation as linearly modulated according to

$$\tilde{\psi}_\sigma(\mathbf{x}) = \psi_\sigma(\mathbf{x}) \left( 1 + A_{\mathcal{R}} \frac{r}{r_{\text{LS}}} \cos \theta \right). \quad (16)$$

For  $\Lambda\text{CDM}$ , we find numerically that  $T^{-1}(k)dT(k)/d(kr_{\text{LS}}) \lesssim 3 \times 10^{-3}$  on all scales, so

that indeed it will be a very good approximation to use Eq. (16), which will simplify the calculations tremendously.

Equation (16) makes it very easy to determine the effect of the modulation on large-scale anisotropies. Those anisotropies take the form

$$\frac{\tilde{\delta T}(\hat{\mathbf{n}})}{T} = \tilde{S}(t_{\text{LS}}, r_{\text{LS}}\hat{\mathbf{n}}), \quad (17)$$

for direction  $\hat{\mathbf{n}}$  and where  $t_{\text{LS}}$  is the time of last scattering, and the source function  $\tilde{S}(t_{\text{LS}}, r_{\text{LS}}\hat{\mathbf{n}})$  is determined fully by  $\tilde{\psi}_\sigma$  and its first and second derivatives (see, e.g., [35]). We have just shown that the linear modulation of  $\mathcal{R}$  corresponds to very good approximation to the linear modulation of the  $\psi_\sigma$  part of  $S(t_{\text{LS}}, r_{\text{LS}}\hat{\mathbf{n}})$ . Next we will examine each derivative term. The first spatial derivative takes the form of a radial derivative:

$$\frac{1}{a_{\text{LS}}H_{\text{LS}}} \frac{\partial}{\partial r} \tilde{\psi}_\sigma(\mathbf{x}) = \frac{1}{a_{\text{LS}}H_{\text{LS}}} \frac{\partial \psi_\sigma(\mathbf{x})}{\partial r} \left( 1 + A_{\mathcal{R}} \frac{r}{r_{\text{LS}}} \cos \theta \right) + \psi_\sigma(\mathbf{x}) A_{\mathcal{R}} \frac{1}{a_{\text{LS}}H_{\text{LS}}r_{\text{LS}}} \cos \theta. \quad (18)$$

The second term on the right-hand side of this expression shows, interestingly, that the derivative of the modulation gives a term degenerate with the modulation of  $\psi_\sigma$  itself. However, for  $\Lambda\text{CDM}$  we have  $a_{\text{LS}}H_{\text{LS}}r_{\text{LS}} = 66.4$ , so that this degenerate term can be ignored (for sources near  $r_{\text{LS}}$ ) and the first derivative of the linearly modulated field  $\tilde{\psi}_\sigma$  can be well approximated by the linear modulation of the derivative of  $\psi_\sigma$ .

The second spatial derivative takes the form of a Laplacian. In this case, it is trivial that the Laplacian commutes with the modulation in Eq. (16), due to the assumed linear nature of the modulation. The same is true for the time derivatives, since the modulation is taken to be time independent, as discussed in Sec. II. Therefore, the temperature anisotropies, Eq. (17), become to a good approximation

$$\frac{\tilde{\delta T}(\hat{\mathbf{n}})}{T} = S(t_{\text{LS}}, r_{\text{LS}}\hat{\mathbf{n}}) (1 + A_{\mathcal{R}} \cos \theta) \quad (19)$$

$$= \frac{\delta T(\hat{\mathbf{n}})}{T} (1 + A_{\mathcal{R}} \cos \theta). \quad (20)$$

In words, the modulated anisotropies are simply given by the anisotropies calculated from the statistically isotropic (“equatorial”) fields, i.e.  $S(t_{\text{LS}}, r_{\text{LS}}\hat{\mathbf{n}})$ , modulated.

This leads directly to the simple temperature multipole covariance of the form studied in [36], i.e. an  $\ell$  to  $\ell \pm 1$  coupling. Expanding Eq. (20) into spherical harmonic multipoles we find

$$\tilde{a}_{\ell m} = a_{\ell m} + A_{\mathcal{R}} \sum_{\ell' m'} a_{\ell' m'} \xi_{\ell m \ell' m'}^0. \quad (21)$$

Here  $\xi_{\ell m \ell' m'}^0$  is the polar component of the coupling coefficients  $\xi_{\ell m \ell' m'}^M$  defined by

$$\xi_{\ell m \ell' m'}^M \equiv \sqrt{\frac{4\pi}{3}} \int Y_{\ell m}^*(\hat{\mathbf{n}}) Y_{\ell' m'}(\hat{\mathbf{n}}) Y_{1M}(\hat{\mathbf{n}}) d\Omega_{\hat{\mathbf{n}}}. \quad (22)$$

Explicitly,

$$\xi_{\ell m \ell' m'}^0 = \delta_{m' m} (\delta_{\ell' \ell-1} A_{\ell-1 m} + \delta_{\ell' \ell+1} A_{\ell m}), \quad (23)$$

$$\xi_{\ell m \ell' m'}^{\pm 1} = \delta_{m' m \mp 1} (\delta_{\ell' \ell-1} B_{\ell-1 \pm m-1} - \delta_{\ell' \ell+1} B_{\ell \mp m}), \quad (24)$$

where

$$A_{\ell m} = \sqrt{\frac{(\ell+1)^2 - m^2}{(2\ell+1)(2\ell+3)}}, \quad (25)$$

$$B_{\ell m} = \sqrt{\frac{(\ell+m+1)(\ell+m+2)}{2(2\ell+1)(2\ell+3)}}. \quad (26)$$

Equation (21) gives a multipole covariance

$$\langle \tilde{a}_{\ell m} \tilde{a}_{\ell' m'}^* \rangle = C_{\ell} \delta_{\ell' \ell} \delta_{m' m} + A_{\mathcal{R}} (C_{\ell} + C_{\ell'}) \xi_{\ell m \ell' m'}^0 \quad (27)$$

to linear order in  $A_{\mathcal{R}}$ , where  $C_{\ell}$  is the power spectrum calculated from  $\mathcal{P}_{\mathcal{R}}^{\text{lo}}(k)$ . This covariance is a complete statistical description of the modulated temperature anisotropies on large scales.

When the scale of the fluctuations sourcing the anisotropies is much smaller than the length scale of variation of the modulation, i.e.  $r_{\text{LS}}$ , then we would expect the effect of the spatial variation of the modulation to be small (see, e.g., [37]). In other words, we expect the  $T$  anisotropies sourced by  $\mathcal{P}_{\mathcal{R}}^{\text{lo}}(k)$  to be modulated to a good approximation according to Eq. (20). Nevertheless, it will be worthwhile to be more quantitative about this expectation, so we examine small scales in detail in the [Appendix](#).

The simple behaviour for small scales (and the detailed calculations in the [Appendix](#)) indicate that to very good approximation the modulated temperature fluctuations on all scales are given by the generalization of Eq. (20):

$$\frac{\tilde{\delta T}(\hat{\mathbf{n}})}{T} \simeq \frac{\delta T^{\text{lo}}(\hat{\mathbf{n}})}{T} (1 + A_{\mathcal{R}} \cos \theta) + \frac{\delta T^{\text{hi}}(\hat{\mathbf{n}})}{T}. \quad (28)$$

Eq. (6) then implies the final result for the multipole covariance:

$$\langle \tilde{a}_{\ell m} \tilde{a}_{\ell' m'}^* \rangle = C_{\ell}^{\Lambda\text{CDM}} \delta_{\ell' \ell} \delta_{m' m} + A_{\mathcal{R}} (C_{\ell}^{\text{lo}} + C_{\ell'}^{\text{lo}}) \xi_{\ell m \ell' m'}^0 \quad (29)$$

to first order in  $A_{\mathcal{R}}$ , where  $C_{\ell}^{\Lambda\text{CDM}}$  is the power spectrum calculated from  $\mathcal{P}_{\mathcal{R}}^{\Lambda\text{CDM}}(k)$  and  $C_{\ell}^{\text{lo}}$  is the spectrum calculated in the same way but using  $\mathcal{P}_{\mathcal{R}}^{\text{lo}}(k)$ .

Notice that the statistical anisotropy in Eq. (29) can be easily calculated using software such as **CAMB** [38] with the primordial spectrum  $\mathcal{P}_{\mathcal{R}}^{\text{lo}}(k)$ . This compares with the approach of [31] who do not make the approximations we have made and hence must calculate some new integrals involving derivatives of internal **CAMB** variables, which is considerably more work. Importantly, note that the form of Eq. (29) is completely general, in that we have the necessary standard  $\Lambda\text{CDM}$  form for the statistically isotropic component, and we have a dipole-modulated part with a scale dependence that is as free as possible, given that it must originate from a  $k$ -space function (in this case  $\mathcal{P}_{\mathcal{R}}^{\text{lo}}(k)$ ). This shows again that our approach

of splitting the primordial fluctuations into uncorrelated low- and high- $k$  parts, while facilitating the calculations, is not restrictive in any way.

We have ignored the ISW effect in this calculation. With the linear modulation model, the modulation amplitude at the redshifts at which the ISW effect is sourced is predicted to be considerably smaller (by a factor  $r_{\text{ISW}}/r_{\text{LS}} \sim 1/5$ ) than the roughly 6% for the primary CMB. Considering also that the ISW signal affects mainly the very largest scales, and that smaller scales are generated at closer distances (recall Fig. 1), it should be a very good approximation to ignore the ISW effect entirely for the asymmetry. That is, the spectrum  $C_{\ell}^{\text{lo}}$  can be calculated without the ISW component. Note also that the effect of the modulated lensing field on the modulated CMB can also be ignored because it is a second-order effect in  $A_{\mathcal{R}}$ .

## B. Connection to general asymmetry form

Using the notation of Ref. [36], the general form for the multipole moment covariance given a polar ( $m=0$ ) modulation can be written

$$\langle \tilde{a}_{\ell m} \tilde{a}_{\ell' m'}^* \rangle = C_{\ell} \delta_{\ell' \ell} \delta_{m' m} + \frac{1}{2} \delta C_{\ell \ell'} \Delta X_0 \xi_{\ell m \ell' m'}^0. \quad (30)$$

The origin of this notation lies in the assumption that the anisotropy power spectrum depends linearly on some parameter,  $X$ , in which case the modulation spectrum,  $\delta C_{\ell \ell'}$ , satisfies

$$\delta C_{\ell \ell'} = \frac{dC_{\ell}}{dX} + \frac{dC_{\ell'}}{dX}. \quad (31)$$

This means that we can formally write down the increment in power between the modulation equator and the poles as

$$\Delta C_{\ell} = \frac{1}{2} \delta C_{\ell \ell} \Delta X_0, \quad (32)$$

where  $\Delta X_0$  is the change in the parameter  $X$  from modulation equator to pole. We will refer to  $\delta C_{\ell \ell'}$  as the statistically anisotropic or modulation power spectrum.

Comparing Eq. (30) to our final result, Eq. (29), we can identify

$$\Delta X_0 = A_{\mathcal{R}} \quad (33)$$

and

$$\delta C_{\ell \ell'} = 2 (C_{\ell}^{\text{lo}} + C_{\ell'}^{\text{lo}}). \quad (34)$$

Equation (32) then allows us to write an effective increment in power between the modulation equator and the poles as

$$\Delta C_{\ell} = 2 A_{\mathcal{R}} C_{\ell}^{\text{lo}}. \quad (35)$$

This is exactly what we would expect, since a fractional modulation of the fluctuation amplitude by  $A_{\mathcal{R}}$  should

result in a modulation of power by  $2A_{\mathcal{R}}$ . This also justifies the approach for calculating the modulated  $\ell$ -space spectra of Ref. [29].

Note that if there is a significant contribution of  $\mathcal{P}_{\mathcal{R}}^{\text{hi}}(k)$  to the lowest  $\ell$ 's, then according to Eq. (35) the actual predicted asymmetry,  $\Delta C_{\ell}/(C_{\ell}^{\text{lo}} + C_{\ell}^{\text{hi}})$ , will be smaller than  $2A_{\mathcal{R}}$ . This is why we said we had in mind that  $\mathcal{P}_{\mathcal{R}}^{\text{hi}}(k)$  would have a negligible contribution to the largest scales: when this is the case our parameter  $2A_{\mathcal{R}}$  will agree well with the actual large-scale asymmetry,  $\Delta C_{\ell}/(C_{\ell}^{\text{lo}} + C_{\ell}^{\text{hi}})$ .

#### IV. EFFECT ON LENSING POTENTIAL

In this section we calculate the effect of a linear modulation of the primordial fluctuations,  $\mathcal{R}$ , on the lensing

potential. The (modulated) lensing potential is determined by a line of sight integral,

$$\tilde{\psi}^{\text{lens}}(\hat{\mathbf{n}}) = -2 \int_0^{r_{\text{LS}}} dr \frac{r_{\text{LS}} - r}{r_{\text{LS}} r} \tilde{\psi}_{\sigma}(t(r), r\hat{\mathbf{n}}) \quad (36)$$

(see, e.g., [39]). Inserting Eq. (16), which we have shown to be an extremely good approximation for the form of the modulated zero-shear gauge fluctuations, and using Eq. (12), an expansion in spherical harmonics and Bessel functions gives

$$\tilde{\psi}^{\text{lens}}(\hat{\mathbf{n}}) = \frac{6}{5} \sqrt{\frac{2}{\pi}} \int_0^{r_{\text{LS}}} dr \frac{r_{\text{LS}} - r}{r_{\text{LS}} r} g(t(r)) \int_0^{\infty} dk k T(k) \sum_{\ell m} \left[ \mathcal{R}_{\ell m}^{\text{lo}}(k) \left( 1 + A_{\mathcal{R}} \frac{r}{r_{\text{LS}}} \cos \theta \right) + \mathcal{R}_{\ell m}^{\text{hi}}(k) \right] j_{\ell}(kr) Y_{\ell m}(\hat{\mathbf{n}}), \quad (37)$$

where  $g(t)$  is the growth suppression factor due to late-time dark energy and

$$\mathcal{R}_{\ell m}(k) \equiv i^{\ell} k \int d\Omega_k \mathcal{R}(\mathbf{k}) Y_{\ell m}^*(\hat{\mathbf{k}}). \quad (38)$$

Therefore the lensing potential multipole moments are

$$\begin{aligned} \psi_{\ell m}^{\text{lens}} &= \frac{6}{5} \sqrt{\frac{2}{\pi}} \int_0^{r_{\text{LS}}} dr \frac{r_{\text{LS}} - r}{r_{\text{LS}} r} g(t(r)) \int_0^{\infty} dk k T(k) \mathcal{R}_{\ell m}(k) j_{\ell}(kr) \\ &+ \frac{6}{5} \sqrt{\frac{2}{\pi}} A_{\mathcal{R}} \int_0^{r_{\text{LS}}} dr \frac{r_{\text{LS}} - r}{r_{\text{LS}} r} g(t(r)) \frac{r}{r_{\text{LS}}} \int_0^{\infty} dk k T(k) \sum_{\ell' m'} \mathcal{R}_{\ell' m'}^{\text{lo}}(k) j_{\ell'}(kr) \xi_{\ell m \ell' m'}^0. \end{aligned} \quad (39)$$

Note the anisotropic part of Eq. (39), which contains the  $r/r_{\text{LS}}$  weighting factor. Finally, we can write the lensing multipole covariance to  $\mathcal{O}(A_{\mathcal{R}})$ ,

$$\begin{aligned} \langle \psi_{\ell m}^{\text{lens}} \psi_{\ell' m'}^{\text{lens}*} \rangle &= \frac{144\pi}{25} \int_0^{\infty} \frac{dk}{k} T^2(k) \mathcal{P}_{\mathcal{R}}^{\Lambda\text{CDM}}(k) \left[ \int_0^{r_{\text{LS}}} dr \frac{r_{\text{LS}} - r}{r_{\text{LS}} r} g(t(r)) j_{\ell}(kr) \right]^2 \delta_{\ell' \ell} \delta_{m' m} \\ &+ \left[ \frac{144\pi}{25} A_{\mathcal{R}} \int_0^{\infty} \frac{dk}{k} T^2(k) \mathcal{P}_{\mathcal{R}}^{\text{lo}}(k) \int_0^{r_{\text{LS}}} dr \frac{r_{\text{LS}} - r}{r_{\text{LS}} r} g(t(r)) j_{\ell}(kr) \int_0^{r_{\text{LS}}} dr' \frac{r_{\text{LS}} - r'}{r_{\text{LS}}^2} g(t(r')) j_{\ell'}(kr') \right. \\ &\left. + (\ell \leftrightarrow \ell') \right] \xi_{\ell m \ell' m'}^0. \end{aligned} \quad (40)$$

Using the general definition for the multipole moment covariance given a polar ( $m = 0$ ) modulation, Eq. (30), we can identify the statistically isotropic part to be

$$C_{\ell} = C_{\ell}^{\text{lens}} = \frac{144\pi}{25} \int_0^{\infty} \frac{dk}{k} T^2(k) \mathcal{P}_{\mathcal{R}}^{\Lambda\text{CDM}}(k) \left[ \int_0^{r_{\text{LS}}} dr \frac{r_{\text{LS}} - r}{r_{\text{LS}} r} g(t(r)) j_{\ell}(kr) \right]^2, \quad (41)$$

while the statistically anisotropic part is

$$\delta C_{\ell \ell'}^{\text{lens}} = \frac{288\pi}{25} \int_0^{\infty} \frac{dk}{k} T^2(k) \mathcal{P}_{\mathcal{R}}^{\text{lo}}(k) \int_0^{r_{\text{LS}}} dr \frac{r_{\text{LS}} - r}{r_{\text{LS}} r} g(t(r)) j_{\ell}(kr) \int_0^{r_{\text{LS}}} dr' \frac{r_{\text{LS}} - r'}{r_{\text{LS}}^2} g(t(r')) j_{\ell'}(kr') + (\ell \leftrightarrow \ell'), \quad (42)$$

with  $\Delta X_0$  again given by Eq. (33). The isotropic part,  $C_{\ell}^{\text{lens}}$ , agrees with the standard result [39], while the

anisotropic part,  $\delta C_{\ell\ell'}^{\text{lens}}$ , is new. It can be easily calculated numerically for  $\Lambda$ CDM transfer function  $T(k)$  and growth function,  $g(t)$ , given a modulation spectrum  $\mathcal{P}_{\mathcal{R}}^{\text{lo}}(k)$ . Note that unlike the case of the primary CMB anisotropies, for lensing the anisotropic part is *not* simply the usual lensing spectrum calculated with  $\mathcal{P}_{\mathcal{R}}^{\text{lo}}(k)$ . The fact that lensing is sourced all along the line of sight means that, instead, the last integral in Eq. (42) is weighted by a factor of  $r/r_{\text{LS}}$ , which reflects the linear nature of the assumed modulation. As anticipated, this reduces the amplitude of the lensing asymmetry relative to that of the primary CMB. The shift to larger angular scales expected for the more closely sourced lensing potential is also encoded in Eq. (42).

We stress that this lensing calculation is considerably simpler than that for the temperature fluctuations, due to the simpler relevant transfer function and simpler dependence of the lensing potential on the primordial fluctuations. Indeed, the only approximation made here is that of Eq. (16), which we have shown to be extremely accurate.

To complete our description of lensing modulation, we can again formally write down the increment in power between the modulation equator and the poles as

$$\Delta C_{\ell}^{\text{lens}} = \frac{1}{2} A_{\mathcal{R}} \delta C_{\ell\ell}^{\text{lens}}. \quad (43)$$

## V. FITTING THE $k$ -SPACE MODULATION TO TEMPERATURE DATA

### A. Formalism

Next we describe how we fit the  $k$ -space modulation spectrum  $\mathcal{P}_{\mathcal{R}}^{\text{lo}}(k)$ , which we have assumed to take the tanh form of Eq. (9), to CMB temperature data. The spectrum depends on two free parameters:  $k_c$  determines which scales are modulated, and  $\Delta \ln k$  determines the sharpness of the transition from modulated to statistically isotropic scales. We denote these parameters by  $p_i = \{k_c, \Delta \ln k\}$ , for brevity. We begin with the likelihood function for the CMB temperature multipoles given the modulation parameters,

$$\mathcal{L}(\mathbf{d}|\Delta X_M, p_i) \propto \frac{1}{\sqrt{|C|}} \exp\left(-\frac{1}{2} \mathbf{d}^\dagger C^{-1} \mathbf{d}\right). \quad (44)$$

Here  $\mathbf{d}$  is the vector of multipole moments and the dependence on the model parameters  $(\Delta X_M, p_i)$  is contained in the multipole covariance matrix  $C$ . Previously we had taken the modulation direction to coincide with the  $\hat{z}$  direction, but now we must keep the direction free and fit for it. Hence the covariance matrix, Eq. (30), becomes [3]

$$C_{\ell m \ell' m'} \equiv \langle \tilde{a}_{\ell m} \tilde{a}_{\ell' m'}^* \rangle \quad (45)$$

$$= C_{\ell} \delta_{\ell' \ell} \delta_{m' m} + \frac{1}{2} \delta C_{\ell\ell'} \sum_M \Delta X_M \xi_{\ell m \ell' m'}^M. \quad (46)$$

The three model parameters  $\Delta X_M$  determine the amplitude and direction of the modulation (see Eqs. (50)–(52) below), while the two modulation parameters  $p_i$  determine the scale dependence of the modulation via Eq. (34), and so we have in total five parameters which describe the statistical anisotropy (we hold the main cosmological parameters fixed).

For fixed  $p_i$ , we can find the  $\Delta X_M$  which maximize the likelihood from Eq. (44) to first order in  $A_{\mathcal{R}}$ . Specifically, for dipole modulation, we use the estimator from [3], which generalizes that of [36] (see Ref. [37] for related optimal estimators):

$$\Delta \tilde{X}_0 = \frac{6}{f_{10}} \frac{\sum_{\ell m} \delta C_{\ell\ell+1} A_{\ell m} S_{\ell m \ell+1 m}}{\sum_{\ell} \delta C_{\ell\ell+1}^2 (\ell+1) F_{\ell} F_{\ell+1}}, \quad (47)$$

$$\Delta \tilde{X}_1 = \frac{6}{f_{11}} \frac{\sum_{\ell m} \delta C_{\ell\ell+1} B_{\ell m} S_{\ell m \ell+1 m+1}}{\sum_{\ell} \delta C_{\ell\ell+1}^2 (\ell+1) F_{\ell} F_{\ell+1}}, \quad (48)$$

and  $\Delta \tilde{X}_{-1} = -\Delta \tilde{X}_1^*$ . Here

$$S_{\ell m \ell' m'} \equiv T_{\ell m}^* T_{\ell' m'} - \langle T_{\ell m}^* T_{\ell' m'} \rangle, \quad (49)$$

where the  $T_{\ell m}$  are  $C$ -inverse filtered temperature multipoles and  $F_{\ell}$  is the mean power spectrum of the  $T_{\ell m}$ . The expectation value in Eq. (49) is an average over a set of realistic simulations, which provides a mean-field correction (described in great detail in [3, 40, 41]). The  $f_{1M}$  factor corrects for normalization errors introduced by masking (its explicit form can be seen in [3]). The  $C$ -inverse filter is identical to that used in [3, 40, 41], and optimally accounts for masking effects. In practice, we bin the estimator, Eqs. (47) and (48), into bins of width  $\Delta \ell = 1$ , which means that the corrections to the data described above only need to be calculated once. This gives exactly the same result as if the estimators were computed for each set of  $p_i$  from scratch; however, it allows us to dramatically speed up the exploration of the parameter space (this technique was also employed in [13] for the same reasons). In the following subsection we describe the data and corresponding simulations used for obtaining these estimators. Given these estimates of the  $\Delta X_M$ , we can write the best-fit amplitude and direction as

$$\tilde{A}_{\mathcal{R}} = \sqrt{\Delta \tilde{X}_0^2 + 2|\Delta \tilde{X}_1|^2}, \quad (50)$$

$$\tilde{\theta} = \cos^{-1} \left( \frac{\Delta \tilde{X}_0}{\tilde{A}_{\mathcal{R}}} \right), \quad (51)$$

$$\tilde{\phi} = -\tan^{-1} \left[ \frac{\text{Im}(\Delta \tilde{X}_1)}{\text{Re}(\Delta \tilde{X}_1)} \right]. \quad (52)$$

The central limit theorem suggests that the  $\Delta X_M$  will be Gaussian distributed (this has been verified explicitly with the use of simulations), and specifically for statistically isotropic skies they will have mean zero. Their variances can be calculated exactly from Eqs. (47) and (48) to be

$$\sigma_X^2(p_i) \equiv \langle |\Delta X_M^2| \rangle = \frac{12}{\sum_{\ell} (\ell+1) \delta C_{\ell\ell+1}^2 C_{\ell}^{-1} C_{\ell+1}^{-1}}. \quad (53)$$



The posterior for the  $\Delta X_M$  parameters for a fixed  $p_i = \bar{p}_i$  is then given by

$$P(\Delta X_M, \bar{p}_i | \mathbf{d}) = \frac{1}{(2\pi)^{3/2} \sigma_X^3} \times \exp \left[ -\frac{\sum_M |\Delta X_M - \tilde{\Delta X}_M|^2}{2\sigma_X^2} \right]. \quad (54)$$

Using these relations, we can evaluate the log-likelihood function at the maximum-likelihood values  $\tilde{\Delta X}_M$  to be

$$\ln \mathcal{L}(\mathbf{d} | \tilde{\Delta X}_M, p_i) = \sum_M \frac{|\tilde{\Delta X}_M|^2}{2\sigma_X^2}, \quad (55)$$

to first order in  $A_{\mathcal{R}}$  and ignoring terms independent of the statistical anisotropy. This tells us that the expectation of the log-likelihood in statistically isotropic skies is independent of  $p_i$ . It also says that the expected increase of the log-likelihood coming from the introduction of the  $\Delta X_M$  parameters is 3, as expected. Note also that this relation means that the likelihood will be very simple to evaluate numerically.

Bayes' theorem allows us to write the posterior for the model parameters as

$$P(\Delta X_M, p_i | \mathbf{d}) = \mathcal{L}(\mathbf{d} | \Delta X_M, p_i) P(\Delta X_M, p_i), \quad (56)$$

with prior  $P(\Delta X_M, p_i)$  on the model parameters, up to an overall normalization. We can calculate the posterior marginalized over the  $\Delta X_M$ 's, with the result

$$P(p_i | \mathbf{d}) \propto \sigma_X^3 \mathcal{L}(\mathbf{d} | \tilde{\Delta X}_M, p_i) P(p_i). \quad (57)$$

Equation (55) then tells us that a natural choice for the prior on the  $p_i$  is

$$P(p_i) \propto \sigma_X^{-3}, \quad (58)$$

which yields an expectation of a flat posterior  $P(p_i | \mathbf{d})$  in statistically isotropic skies. Hence this is the prior we choose. We also choose a flat prior in the  $\Delta X_M$ 's, as is usually done.

Once the best-fit modulation spectrum parameters  $(k_c, \Delta \ln k)$  are found, it will be a simple matter to evaluate the lensing asymmetry using the method laid out in Sec. IV, and, in the future, the polarization asymmetry as well.

## B. Results

The results presented here are based on the component-separated temperature maps provided by the Planck Collaboration [42]. Namely, we use the **Commander**, **NILC**, **SEVEM**, and **SMICA** 2015 temperature maps [43] at a **HEALPix** [44] resolution of  $N_{\text{side}} = 2048$  (for brevity we only quote the results for **SMICA**; however, we have checked that the other maps do not give substantially different results). We also use the UT78

mask provided by the Planck Collaboration, referred to as the common mask. We use a set of 1000 FFP8 simulations [50][45], corresponding to each component separation method, in order to make mean-field and normalization corrections to the data, as was done in [3].

Using the relations of Eqs. (50)–(52), we can perform a one-to-one linear transformation from the  $\Delta X_M$  to Cartesian modulation components,  $\{\Delta X, \Delta Y, \Delta Z\}$ . The  $\{\Delta X, \Delta Y, \Delta Z\}$  are simply the components of the dipole modulation vector in Cartesian Galactic coordinates. In what follows we will present results in this coordinate system for convenience. We scan the model space over the following parameter ranges:  $\ln(k_c [\text{Mpc}^{-1}]) \in [-7.2, -3.2]$ ,  $\Delta \ln k \in [0.01, 0.5]$ , and  $|\Delta X|, |\Delta Y|, |\Delta Z| \leq 1$ . The lower limit on  $k_c$  is placed to ensure that we only look for modulation on scales that are observable, while the lower limit on  $\Delta \ln k$  corresponds essentially to an abrupt cutoff in  $k$  space. The upper limits on  $k_c$  and  $\Delta \ln k$  are somewhat arbitrary: in multipole space they correspond approximately to limiting the modulation to  $\ell < 1000$ . We are primarily interested in large-scale modulations, and previous  $\ell$ -space results [3, 9–11] indicated no evidence for modulation on scales smaller than this limit. For  $A_{\mathcal{R}} > 1$  the fluctuations in Eq. (4) will go to zero somewhere within our last scattering surface, and the details of the modulation in this case will depend on the specific modulation mechanism. For the tanh model we do not approach this regime: the limits on the modulation amplitude components turn out to be generous. We explore the parameter space using a simple grid approach, which is adequate since the parameter space is effectively only two dimensional via Eq. (54).

Results are summarized as the posterior of the full parameter set  $\{k_c, \Delta \ln k, \Delta X, \Delta Y, \Delta Z\}$  in Fig. 2. We also present results for a condensed version of the parameter space, i.e. the set  $\{k_c, \Delta \ln k, A_{\mathcal{R}}\}$ , where the angular variables have been marginalized over, in Fig. 3. We can see from the distributions that no parameter is constrained very well. In particular,  $\Delta \ln k$  is completely unconstrained by the data, which suggests that there is no well-defined transition in the data between modulated and unmodulated scales. This is not surprising, since we have opened up the parameter space in our formalism with respect to most previous studies, which considered a sharp cutoff in  $\ell$  space and only found apparently significant modulation when that cutoff was fixed. In Table I we quote the mean value parameters and their uncertainties, which we take as the mean of the marginalized posteriors and the area that encloses 68% of the likelihood. We also quote the maximum-likelihood parameters. For comparison, when testing for an  $\ell$ -space modulation to  $\ell = 65$ , Ref. [3] found  $A_{\mathcal{R}} = 0.062^{+0.026}_{-0.013}$  in the direction  $(l, b) = (213^\circ, -26^\circ) \pm 28^\circ$ .

The temperature anisotropy modulation spectrum  $C_\ell^{\text{lo}}$  and effective power spectrum difference from modulation equator to pole,  $\Delta C_\ell$ , for the maximum-likelihood modulation parameters from Table I, are plotted in Fig. 4. These were calculated using CAMB with the correspond-

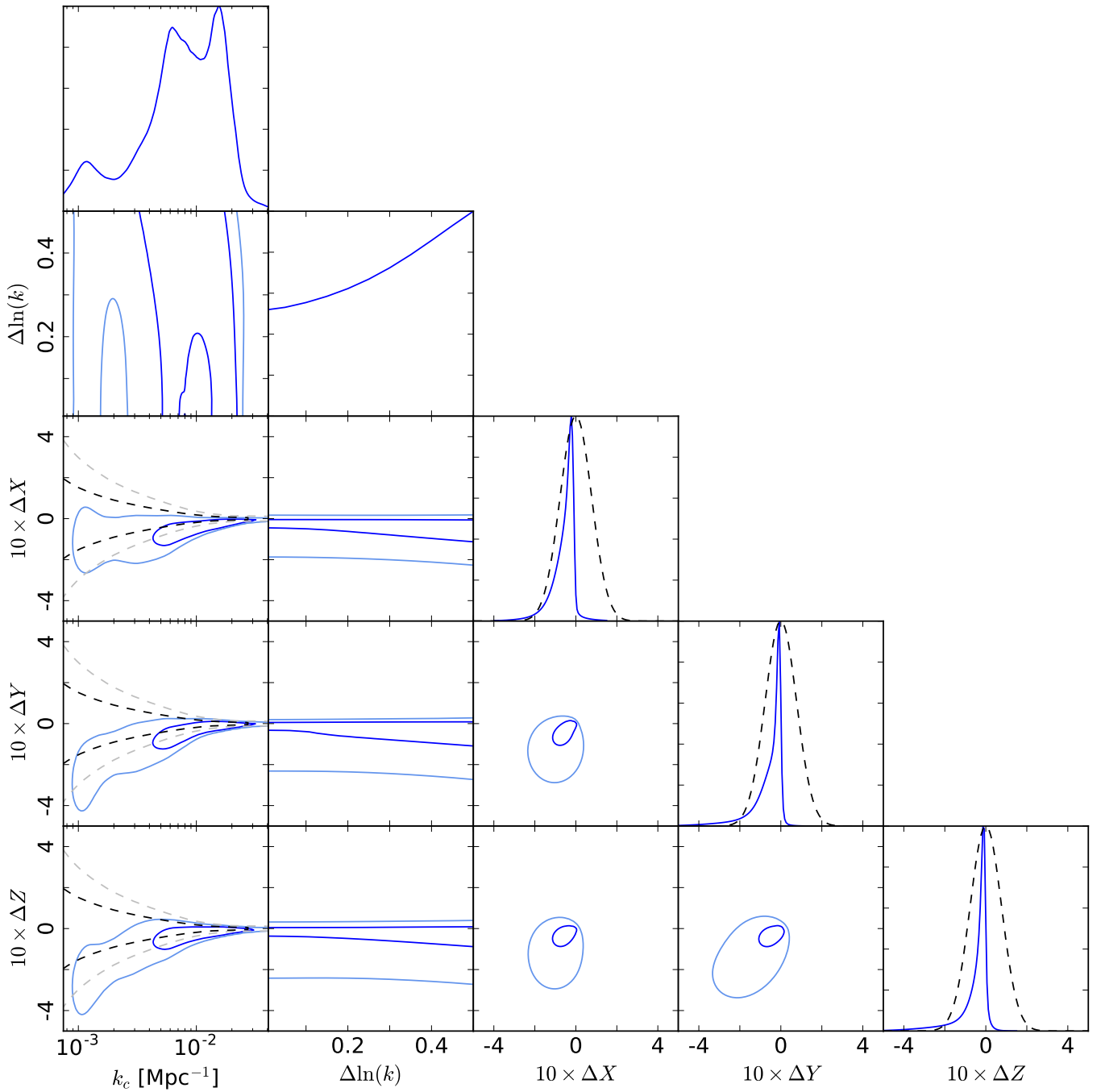


FIG. 2: Marginalized posteriors for the parameter set  $\{p_i, \Delta X, \Delta Y, \Delta Z\}$ ; dark and light blue (solid) contours enclose 68% and 95% of the likelihood, respectively. The black and grey (dashed) contours and curves represent the theoretical distributions of the parameters coming solely from cosmic variance in statistically isotropic skies. The values  $(k_c, \Delta \ln k) = (5 \times 10^{-3} \text{ Mpc}^{-1}, 0)$  would correspond roughly to the often-considered  $\ell$ -space modulation to  $\ell \simeq 65$ .

ing best-fit primordial spectrum  $\mathcal{P}_{\mathcal{R}}^{\text{lo}}(k)$  and setting the ISW source to zero for redshifts  $z < 30$ . (Negligible differences were found when the ISW effect was included in the anisotropic spectrum.) The modulation in amplitude is at a level of roughly 7% to  $\ell \simeq 50$ . Importantly, while this agrees crudely with the often-quoted level of 6–7% to  $\ell \simeq 65$ , we stress that the temperature asymmetry is poorly constrained: the  $k_c$  posterior in Figs. 2 and

3 has significant weight over a large range of values, corresponding to  $\ell \simeq 50$ –250. As the  $k_c$ - $\mathcal{A}_{\mathcal{R}}$  panel in Fig. 3 shows, these two parameters are anticorrelated, with a larger  $k_c$  implying a smaller  $\mathcal{A}_{\mathcal{R}}$ . Furthermore, as the dashed contours in that panel show, this anticorrelation follows the trend expected from cosmic variance, which arises simply because larger  $k_c$  implies more modes and hence lower cosmic variance. This poorly-defined char-

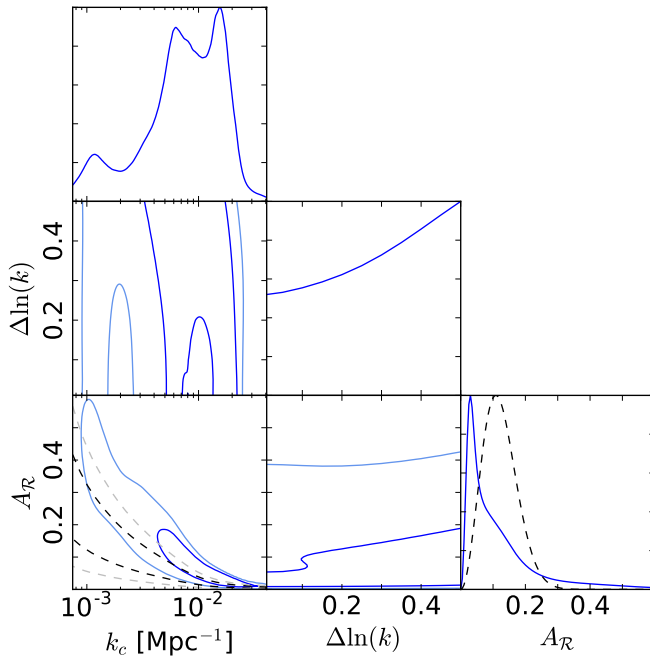


FIG. 3: Marginalized posteriors for the parameter set  $\{p_i, A_R\}$ ; dark and light blue (solid) contours enclose 68% and 95% of the likelihood, respectively. The black and grey (dashed) contours and curve represent the theoretical distributions of the parameters coming solely from cosmic variance in statistically isotropic skies.

Parameter	Mean value	Max likelihood
$10^3 k_c [\text{Mpc}^{-1}]$	$7.08^{+12.56}_{-2.34}$	7.83
$\Delta \ln k$	unconstrained	0.5
$\Delta X$	$-0.060^{+0.054}_{-0.018}$	-0.0610
$\Delta Y$	$-0.063^{+0.069}_{-0.010}$	-0.0414
$\Delta Z$	$-0.056^{+0.062}_{-0.004}$	-0.0347
$A_R$	$0.122^{+0.014}_{-0.112}$	0.0871
$l [^\circ]$	$224^{+43}_{-44}$	214
$b [^\circ]$	$-31^{+31}_{-16}$	-25
$A_R$	$0.095^{+0.026}_{-0.080}$	...

TABLE I: Marginalized posterior mean values and their 68% uncertainties for the modulation parameters of the model of Eq. (9), along with their corresponding maximum-likelihood values. The angles  $l$  and  $b$  are the Galactic longitude and latitude, respectively, calculated via Eqs. (51) and (52). The final row is the combined constraint including an ideal CMB lensing experiment assuming a modulation with amplitude  $A_R = 0.122$  and the remaining temperature mean values. The addition of lensing does not appreciably help to constrain the model.

acter of the asymmetry may be surprising, but has previously been found in  $\ell$  space (see in particular the peaks at  $\ell \simeq 200$ – $300$  in figure 30 of [3] and figure 15 of [2], which have similar significance to the peaks at  $\ell \simeq 65$ ).

Finally, note that Fig. 4 shows that an origin to the  $T$  asymmetry as a modulation of the ISW effect alone

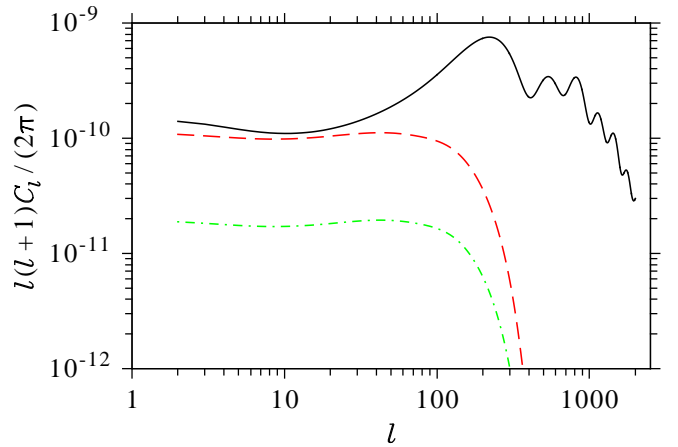


FIG. 4: Temperature anisotropy isotropic power spectrum,  $C_\ell^{\Lambda\text{CDM}}$  (solid black curve), anisotropic power spectrum,  $C_\ell^{\text{lo}}$  (dashed red curve), and power spectrum increment from equator to pole,  $\Delta C_\ell$  (dot-dashed green curve), for the case of the maximum-likelihood modulation from Table I, which fits the observed temperature asymmetry. The modulation in amplitude is at a level of roughly 7% to  $\ell \simeq 50$ .

(perhaps via an anisotropic sound speed for dark energy) is unlikely to produce a good fit to the data, since the ISW contribution is extremely weak for  $\ell \gtrsim 50$ .

## VI. PREDICTIONS FOR CMB LENSING

### A. Modulation power spectrum

Having used the CMB temperature data to fit the  $k$ -space modulation spectrum,  $\mathcal{P}_R^{\text{lo}}(k)$ , in the last section, we are now ready to present the prediction for the CMB lensing asymmetry. Once the fitting has been done, we know the modulation direction via the  $\Delta \tilde{X}_M$ , and so we can write the multipole covariance as Eq. (30) with the polar direction along the modulation direction and amplitude  $A_R$ .

Using the maximum-likelihood  $k$ -space modulation spectrum parameters,  $k_c$ ,  $\Delta \ln k$ , and  $\Delta \tilde{X}_M$ , from Table I, we calculated the statistically anisotropic lensing spectrum,  $\delta C_\ell^{\text{lens}}$ , using Eq. (42). The result is plotted in Fig. 5. The lensing spectrum is modulated at a level of about 3% and less in power (about 1.5% and less in amplitude), out to scales as small as  $\ell \simeq 50$ . As predicted in Sec. I on geometrical grounds, the lensing potential is modulated to a larger minimum angular scale and by a smaller amplitude than the corresponding temperature best fit presented in Fig. 4. This directly leads to a low modulation detection significance for lensing, as we will see in the next subsection.

Note that the anisotropic spectrum grows relative to the isotropic spectrum at large to intermediate scales. This can be understood with the help of Fig. 1, where it is apparent that larger lensing multipoles are typically sourced at greater distances. For our assumed linear

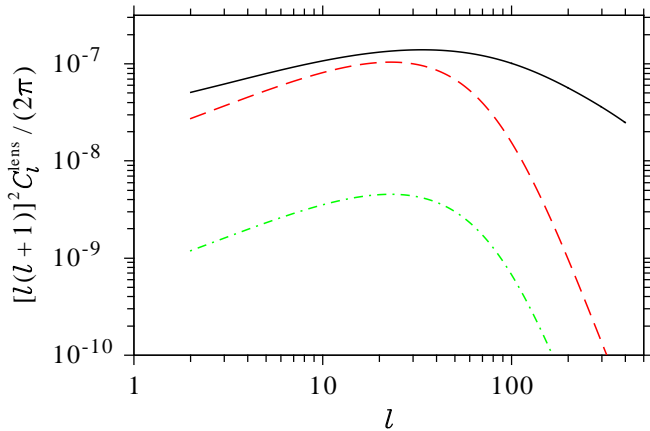


FIG. 5: Lensing potential isotropic power spectrum,  $C_\ell^{\text{lens}}$  (black curve), predicted anisotropic power spectrum,  $\delta C_{\ell\ell}^{\text{lens}}$  (red curve), and predicted power spectrum increment from equator to pole,  $\Delta C_\ell^{\text{lens}}$  (green curve), for the case of the maximum-likelihood modulation from Table I, which fits the observed temperature asymmetry. The modulation in amplitude is at a level of roughly 1.5% or less to  $\ell \simeq 50$ .

modulation form, larger distances, and hence larger multipoles, will be modulated with larger amplitude. Compared with this lensing case, the corresponding temperature anisotropy spectrum in Fig. 4 exhibits a much more similar shape to the isotropic spectrum, up to the cut-off  $k_c$  and allowing for the lack of the ISW contribution in the anisotropic spectrum. This is simply due to the fact that the primary CMB is sourced at essentially a single distance,  $r_{\text{LS}}$ , and hence is modulated at a single amplitude for our linear model.

### B. Detectability for ideal lensing map

In order to ascertain the detectability of the predicted lensing potential modulation, we must compare the prediction to the expected uncertainty in the measurement. The expected variance of a CMB lensing measurement of asymmetry will be determined by cosmic variance (of the lensing potential modes) and lensing reconstruction noise. It turns out that for a lensing reconstruction based on cosmic-variance-limited temperature and polarization anisotropy measurements, the reconstruction noise is small compared to the lensing potential cosmic variance, at least over the relevant scales [46] [51]. Therefore, an ideal lensing measurement can be considered essentially cosmic variance limited. Realistic lensing experiments will have higher noise which will necessarily reduce our ability to detect a modulation. Hence our conclusions will be conservative.

We can easily evaluate the cosmic variance of the modulation amplitude  $\Delta X_0$  given a lensing modulation spectrum,  $\delta C_{\ell\ell}^{\text{lens}}$ , using Eq. (53). Using Eqs. (33), (41), and (42) for the case of the maximum-likelihood parameters, we find  $\sqrt{\langle A_{\mathcal{R}}^2 \rangle} = 0.111$ . This means that the maximum-likelihood modulation amplitude determined from the  $T$

anisotropies,  $A_{\mathcal{R}} = 0.0871$ , is  $0.0871/0.111 = 0.8$  standard deviations from zero for a lensing measurement along the known  $T$  modulation direction. For the mean value modulation parameters from Table I, we find an expected measurement of  $0.9\sigma$ . However, in this case the highly non-Gaussian posterior (recall Fig. 3) means that the mean value parameters are biased towards high significance. In fact, given the likelihood from temperature we can determine that the mean detection significance for  $A_{\mathcal{R}}$  by lensing is  $0.7\sigma$  and the probability of obtaining a greater than  $1\sigma$  detection of  $A_{\mathcal{R}}$  in lensing is of order 10%. The probability is of order 0.1% for finding a greater than  $1.5\sigma$  detection of  $A_{\mathcal{R}}$  and decreases quite rapidly for higher detection limits. Therefore, even in this case of an ideal, cosmic-variance-limited lensing map, lensing will tell us very little about whether the asymmetry is real or not.

We can illustrate the weakness of CMB lensing for testing a physical modulation in another way. The last row of Table I lists the result of combining the constraint on  $A_{\mathcal{R}}$  from the  $T$  anisotropies with the expected constraint for lensing, assuming a modulation with parameters given by the mean values of Table I, which were determined by the  $T$  likelihood. It is apparent that lensing does not improve the constraint on  $A_{\mathcal{R}}$  significantly. If we consider relaxing the condition here that the  $p_i$  be fixed, we can see that CMB lensing will not be able to constrain the modulation model significantly better than CMB  $T$  alone.

## VII. DISCUSSION

In this paper we have presented a rigorous formalism for describing a linearly modulated primordial fluctuation field in  $k$  space with arbitrary scale dependence, and have calculated its effects on CMB temperature fluctuations as well as the lensing potential, which probes independent modes from the primary CMB. We performed a Bayesian parameter estimation for the  $k$ -space modulation spectrum, fitting to *Planck* temperature data. We then predicted the corresponding CMB lensing modulation, and found that even an ideal lensing experiment would expect to see the modulation at only about  $0.7\sigma$ . Hence it appears that CMB lensing will never tell us much about whether the observed  $T$  modulation is a statistical fluke or is due to a real, physical modulation of the primordial fluctuations. Also, this means that the null result for asymmetry in the *Planck* lensing map [9] is completely unsurprising, given that the *Planck* lensing map contains substantially more noise than an ideal map would.

In principle, correlating CMB lensing with other probes should improve the attainable significance of the expected modulation. However, recall from Fig. 1 that current galaxy surveys have weak sensitivity at the required extremely large scales. In addition, such surveys reach to relatively low redshifts, and hence we would expect a low modulation amplitude, at least for a linear



modulation. Nevertheless, it may be worth considering this more carefully, given our result that the upper limit for the cutoff is near  $k_c \simeq 0.02 \text{ Mpc}^{-1}$ . The ISW contribution reaches to sufficiently large scales, but is sourced so close to us that, again, its modulation amplitude is expected to be very small.

It is important to point out that, although it appears that we cannot usefully probe the asymmetry with CMB lensing, it will still be important to examine lensing maps for departures from statistical isotropy. Lensing probes a large fraction of our observable volume that is inaccessible by other means. Hence it provides a unique opportunity to test the simplest models of fluctuations [25].

Our results also highlight a seldom-stressed aspect of the temperature asymmetry. We found that no well-defined  $k$ -space modulation exists, and instead that the modulation cutoff scale,  $k_c$ , is only weakly constrained. In particular, there is no reason to single out an approximately 6% modulation to  $\ell \simeq 65$ . However, this poor constraint means that our results should be only weakly sensitive to our choice for  $\mathcal{P}_{\mathcal{R}}^{\text{lo}}(k)$ , i.e. to departures from the tanh form.

It is clear that polarization will be our best opportunity in the near term to test for a physical modulation. However, even though polarization can sample about as many independent modes as temperature, Ref. [29] finds strong  $k$ -space model dependence for the predictions of polarization. It will be important to examine this with our fitting procedure. In particular, we will need to generalize our approach to incorporate isocurvature and tensor mode modulations.

In the distant future 21-cm surveys may have the ability to reach to large distances and very large scales. They will have, in principle, vastly many more modes within reach via three-dimensional mapping than do the two-dimensional CMB or lensing measurements. Hence they should finally resolve the status of the power asymmetry and other anomalies.

### Acknowledgments

We thank Adam Moss and Ali Narimani for useful discussions. This research was supported by the Canadian Space Agency and the Natural Sciences and Engineering Research Council of Canada. We acknowledge the use of the CAMB [38] and HEALpix [44] codes.

*Note added.*—After this work was nearly complete, a related study appeared [47], which examines the effect of dipole modulation on lensing. That study apparently predicts considerably larger CMB lensing modulation amplitudes than we find. However, it appears that it ignores the spatial dependence of the modulation, replacing our Eq. (3) with

$$\tilde{\mathcal{R}}^{\text{lo}}(\mathbf{x}) = \mathcal{R}^{\text{lo}}(\mathbf{x}) (1 + A_{\mathcal{R}} \cos \theta). \quad (59)$$

Hence they do not see the large reduction in modulation

amplitude due to the sourcing of lensing at relatively low redshifts. In addition, [47] do not fit a modulation to  $T$  data nor do they predict the detectability for lensing.

### Appendix: Effect on small-scale $T$ anisotropies

As we mentioned in Sec. III A, when the scale of the perturbations sourcing the anisotropies is much smaller than the length scale of variation of the modulation, we expect the effect of the spatial variation of the modulation to be small. Nevertheless, it will be useful to be more quantitative about this expectation.

There are three main changes to the temperature anisotropies calculated in Sec. III A when sources on smaller scales are considered. First, the relevant transfer functions become oscillatory in  $k$  due to the acoustic oscillations. Next, relaxing the tight-coupling approximation means that anisotropic stress must be included. Finally, relaxing the sudden-recombination approximation means that the anisotropies are sourced over a range of redshifts, rather than just at  $z_{\text{LS}}$ . We will consider each of these effects in turn.

To a good approximation, the part of the anisotropy proportional to  $\mathcal{R}$  (sometimes referred to as the “monopole”) takes on a term of order (see, e.g., [48])

$$\cos(kr_s) \mathcal{R}(\mathbf{k}) \equiv T_1(k) \mathcal{R}(\mathbf{k}), \quad (\text{A.1})$$

where  $r_s$  is the sound horizon. This term necessarily approaches  $T(k) \mathcal{R}(\mathbf{k})$  in the large-scale limit. Similarly, the part proportional to the radial derivative of  $\mathcal{R}$  (the “dipole”) becomes of order

$$\sin(kr_s) \mathcal{R}(\mathbf{k}) \equiv T_2(k) \mathcal{R}(\mathbf{k}), \quad (\text{A.2})$$

which again must approach the large-scale limit  $T(k)/(a_{\text{LS}} H_{\text{LS}}) \mathcal{R}(\mathbf{k})$ . Recall that we can consider the linear modulation to commute with the transfer function filtering if Eq. (15) is satisfied. Here we have

$$\left| \frac{1}{T_1(k)} \frac{dT_1(k)}{dkr_{\text{LS}}} \right| = \frac{r_s}{r_{\text{LS}}} \tan(kr_s) \simeq 0.01 \tan(kr_s) \quad (\text{A.3})$$

and

$$\left| \frac{1}{T_2(k)} \frac{dT_2(k)}{dkr_{\text{LS}}} \right| \simeq 0.01 \cot(kr_s). \quad (\text{A.4})$$

Therefore for most  $k$  scales, the condition for commutativity is met. For the dipole term, the cot dependence may suggest a problem as  $k \rightarrow 0$ . However, we showed explicitly in Sec. III A that the dipole term does, in fact, commute to a good approximation with modulation on large scales. Similarly, the periodic divergences in  $\tan(kr_s)$  and  $\cot(kr_s)$  at larger  $k$  values may suggest that commutativity breaks down at these scales. To examine the effect of these divergences, consider the covariance of  $T(k) \tilde{\mathcal{R}}(\mathbf{k})$  calculated using Eq. (13) for  $T(k) = \cos(kr_s)$ . In addition to the expected statistically isotropic term proportional to

$\cos^2(kr_s)\mathcal{P}_{\mathcal{R}}(k)$ , we find an extra isotropic term proportional to  $\cos(kr_s)\sin(kr_s)\mathcal{P}_{\mathcal{R}}(k)r_s/r_{\text{LS}}$ . Very close to the zeros of  $\cos(kr_s)$  this extra term will dominate. However, its *absolute* contribution is weighted by the small factor  $r_s/r_{\text{LS}}$ . The relatively broad kernel that takes us from  $k$  to  $\ell$  space will mean that the extra term will alter the acoustic peak structure only by a small amount, in proportion to the factor  $r_s/r_{\text{LS}}$ . This tells us that the modulation commutes to good approximation with the acoustic oscillation processing.

The next small-scale effect is the presence of anisotropic stress, i.e. the quadrupole Boltzmann terms. These terms are suppressed by factors  $k/|\dot{\tau}| \sim 10^{-3}kr_{\text{LS}}$ , where  $\tau$  is the optical depth (see, e.g., [49]). The anisotropic stress is sourced within distances of the order the mean free path from the observed point on the last scattering surface, which is much smaller than  $r_{\text{LS}}$ , and is determined by gradients of the primordial field. Hence, as we showed for the case of the derivative terms in Sec. III A, for these contributions modulation will commute to a very good approximation with filtering. Importantly, as polarization is sourced entirely by anisotropic stress, this will mean that we will be able to describe in a similar way the effect of modulation on polarization.

The final small-scale effect is the sourcing over a range of redshifts, weighted by the visibility function. Including also the high- $k$  part of the fluctuations, the anisotropy of Eq. (17) becomes in this case the line-of-sight integral

$$\frac{\delta\widetilde{T}(\hat{\mathbf{n}})}{T} = \int_0^\infty dr \left[ \widetilde{S}^{\text{lo}}(t(r), r\hat{\mathbf{n}}) + S^{\text{hi}}(t(r), r\hat{\mathbf{n}}) \right]. \quad (\text{A.5})$$

The previous arguments tell us that, to a good approximation, we can write

$$\widetilde{S}^{\text{lo}}(t(r), r\hat{\mathbf{n}}) \simeq S^{\text{lo}}(t(r), r\hat{\mathbf{n}}) \left( 1 + A_{\mathcal{R}} \frac{r}{r_{\text{LS}}} \cos\theta \right). \quad (\text{A.6})$$

Therefore, writing  $r = r_{\text{LS}} + \delta r$ , the anisotropy becomes

$$\frac{\delta\widetilde{T}(\hat{\mathbf{n}})}{T} \simeq \int_0^\infty dr \left[ S^{\text{lo}}(t(r), r\hat{\mathbf{n}}) (1 + A_{\mathcal{R}} \cos\theta) + S^{\text{hi}}(t(r), r\hat{\mathbf{n}}) \right] + \mathcal{O}(\delta r/r_{\text{LS}}). \quad (\text{A.7})$$

Since the primary anisotropies are sourced over a range of distances  $\delta r/r_{\text{LS}} \sim 10^{-3}$ , we have to very good approximation

$$\frac{\delta\widetilde{T}(\hat{\mathbf{n}})}{T} \simeq \frac{\delta T^{\text{lo}}(\hat{\mathbf{n}})}{T} (1 + A_{\mathcal{R}} \cos\theta) + \frac{\delta T^{\text{hi}}(\hat{\mathbf{n}})}{T}. \quad (\text{A.8})$$

Using Eq. (6), this leads immediately, as in Sec. III A, to the final result for the multipole covariance:

$$\langle \widetilde{a}_{\ell m} \widetilde{a}_{\ell' m'}^* \rangle = C_\ell^{\Lambda\text{CDM}} \delta_{\ell' \ell} \delta_{m' m} + A_{\mathcal{R}} (C_\ell^{\text{lo}} + C_{\ell'}^{\text{lo}}) \xi_{\ell m \ell' m'}^0 \quad (\text{A.9})$$

to first order in  $A_{\mathcal{R}}$ , where  $C_\ell^{\Lambda\text{CDM}}$  is the power spectrum calculated from  $\mathcal{P}_{\mathcal{R}}^{\Lambda\text{CDM}}(k)$  and  $C_\ell^{\text{lo}}$  is the spectrum calculated in the same way but using  $\mathcal{P}_{\mathcal{R}}^{\text{lo}}(k)$ .

- 
- [1] Planck Collaboration, *Astron. Astrophys.* **594**, A13 (2016), arXiv:1502.01589 [astro-ph.CO].
  - [2] C. L. Bennett et al., *Astrophys. J. Suppl.* **192**, 17 (2011), arXiv:1001.4758 [astro-ph.CO].
  - [3] Planck Collaboration, *Astron. Astrophys.* **594**, A16 (2016), arXiv:1506.07135 [astro-ph.CO].
  - [4] D. J. Schwarz, C. J. Copi, D. Huterer, and G. D. Starkman (2015), arXiv:1510.07929 [astro-ph.CO].
  - [5] G. Efstathiou, Y.-Z. Ma, and D. Hanson, *Mon. Not. Roy. Astron. Soc.* **407**, 2530 (2010), arXiv:0911.5399 [astro-ph.CO].
  - [6] A. Rassat, J. L. Starck, and F. X. Dupe, *Astron. Astrophys.* **557**, A32 (2013), arXiv:1303.4727 [astro-ph.CO].
  - [7] A. Rassat and J. L. Starck, *Astron. Astrophys.* **557**, L1 (2013), arXiv:1303.5051 [astro-ph.CO].
  - [8] H. K. Eriksen, F. K. Hansen, A. J. Banday, K. M. Gorski, and P. B. Lilje, *Astrophys. J.* **605**, 14 (2004), [Erratum: *Astrophys. J.* 609, 1198 (2004)], arXiv:astro-ph/0307507 [astro-ph].
  - [9] S. Flender and S. Hotchkiss, *JCAP* **1309**, 033 (2013), arXiv:1307.6069 [astro-ph.CO].
  - [10] M. Quartin and A. Notari, *JCAP* **1501**, 008 (2015), arXiv:1408.5792 [astro-ph.CO].
  - [11] S. Aiola, B. Wang, A. Kosowsky, T. Kahniashvili, and H. Firouzjahi, *Phys. Rev.* **D92**, 063008 (2015), arXiv:1506.04405 [astro-ph.CO].
  - [12] A. L. Erickcek, C. M. Hirata, and M. Kamionkowski, *Phys. Rev.* **D80**, 083507 (2009), arXiv:0907.0705 [astro-ph.CO].
  - [13] Planck Collaboration, *Astron. Astrophys.* **594**, A20 (2016), arXiv:1502.02114 [astro-ph.CO].
  - [14] C. T. Byrnes, D. Regan, D. Seery, and E. R. M. Tarrant, *JCAP* **1606**, 025 (2016), arXiv:1511.03129 [astro-ph.CO].
  - [15] E. Dimastrogiovanni, N. Bartolo, S. Matarrese, and A. Riotto, *Adv. Astron.* **2010**, 752670 (2010), arXiv:1001.4049 [astro-ph.CO].
  - [16] J. Soda, *Class. Quant. Grav.* **29**, 083001 (2012), arXiv:1201.6434 [hep-th].
  - [17] A. Naruko, E. Komatsu, and M. Yamaguchi, *JCAP* **1504**, 045 (2015), arXiv:1411.5489 [astro-ph.CO].
  - [18] F. Schmidt and L. Hui, *Phys. Rev. Lett.* **110**, 011301 (2013), [Erratum: *Phys. Rev. Lett.* 110, 059902 (2013)], arXiv:1210.2965 [astro-ph.CO].
  - [19] L. R. Abramo and T. S. Pereira, *Adv. Astron.* **2010**, 378203 (2010), arXiv:1002.3173 [astro-ph.CO].
  - [20] A. Ashoorioon and T. Koivisto, *Phys. Rev.* **D94**, 043009 (2016), arXiv:1507.03514 [astro-ph.CO].
  - [21] C. Dvorkin, H. V. Peiris, and W. Hu, *Phys. Rev.* **D77**, 063008 (2008), arXiv:0711.2321 [astro-ph].

- [22] F. Paci, A. Gruppuso, F. Finelli, P. Cabella, A. De Rosa, N. Mandolesi, and P. Natoli, *Mon. Not. Roy. Astron. Soc.* **407**, 399 (2010), arXiv:1002.4745 [astro-ph.CO].
- [23] C. J. Copi, D. Huterer, D. J. Schwarz, and G. D. Starkman, *Mon. Not. Roy. Astron. Soc.* **434**, 3590 (2013), arXiv:1303.4786 [astro-ph.CO].
- [24] S. Ghosh, R. Kothari, P. Jain, and P. K. Rath, *JCAP* **1601**, 046 (2016), arXiv:1507.04078 [astro-ph.CO].
- [25] J. P. Zibin and A. Moss (2014), arXiv:1409.3831 [astro-ph.CO].
- [26] C. M. Hirata, *JCAP* **0909**, 011 (2009), arXiv:0907.0703 [astro-ph.CO].
- [27] A. Cimatti, R. Laureijs, B. Leibundgut, S. Lilly, R. Nichol, et al. (2009), arXiv:0912.0914 [astro-ph.CO].
- [28] L. Dai, D. Jeong, M. Kamionkowski, and J. Chluba, *Phys. Rev. D* **87**, 123005 (2013), arXiv:1303.6949 [astro-ph.CO].
- [29] M. H. Namjoo, A. A. Abolhasani, H. Assadullahi, S. Baghram, H. Firouzjahi, and D. Wands, *JCAP* **1505**, 015 (2015), arXiv:1411.5312 [astro-ph.CO].
- [30] P. K. Rath, P. K. Aluri, and P. Jain, *Phys. Rev. D* **91**, 023515 (2015), arXiv:1403.2567 [astro-ph.CO].
- [31] R. Kothari, S. Ghosh, P. K. Rath, G. Kashyap, and P. Jain, *Mon. Not. Roy. Astron. Soc.* **460**, 1577 (2016), arXiv:1503.08997 [astro-ph.CO].
- [32] S. Mukherjee and T. Souradeep, *Phys. Rev. Lett.* **116**, 221301 (2016), arXiv:1509.06736 [astro-ph.CO].
- [33] C. Li, T. L. Smith, and A. Cooray, *Phys. Rev. D* **75**, 083501 (2007), arXiv:astro-ph/0607494 [astro-ph].
- [34] N. Kaiser and A. H. Jaffe, *Astrophys. J.* **484**, 545 (1997), arXiv:astro-ph/9609043 [astro-ph].
- [35] J. P. Zibin and D. Scott, *Phys. Rev. D* **78**, 123529 (2008), arXiv:0808.2047 [astro-ph].
- [36] A. Moss, D. Scott, J. P. Zibin, and R. Battye, *Phys. Rev. D* **84**, 023014 (2011), arXiv:1011.2990 [astro-ph.CO].
- [37] D. Hanson and A. Lewis, *Phys. Rev. D* **80**, 063004 (2009), arXiv:0908.0963 [astro-ph.CO].
- [38] A. Lewis, A. Challinor, and A. Lasenby, *Astrophys. J.* **538**, 473 (2000), arXiv:astro-ph/9911177 [astro-ph].
- [39] A. Lewis and A. Challinor, *Phys. Rept.* **429**, 1 (2006), arXiv:astro-ph/0601594 [astro-ph].
- [40] Planck Collaboration, *Astron. Astrophys.* **571**, A17 (2014), arXiv:1303.5077 [astro-ph.CO].
- [41] Planck Collaboration, *Astron. Astrophys.* **594**, A15 (2016), arXiv:1502.01591 [astro-ph.CO].
- [42] Planck Collaboration, *Astron. Astrophys.* **594**, A1 (2016), arXiv:1502.01582 [astro-ph.CO].
- [43] Planck Collaboration, *Astron. Astrophys.* **594**, A9 (2016), arXiv:1502.05956 [astro-ph.CO].
- [44] K. M. Gorski, E. Hivon, A. J. Banday, B. D. Wandelt, F. K. Hansen, M. Reinecke, and M. Bartelman, *Astrophys. J.* **622**, 759 (2005), arXiv:astro-ph/0409513 [astro-ph].
- [45] Planck Collaboration, *Astron. Astrophys.* **594**, A12 (2016), arXiv:1509.06348 [astro-ph.CO].
- [46] J. Lesgourgues, L. Perotto, S. Pastor, and M. Piat, *Phys. Rev. D* **73**, 045021 (2006), arXiv:astro-ph/0511735 [astro-ph].
- [47] F. Hassani, S. Baghram, and H. Firouzjahi, *JCAP* **1605**, 044 (2016), arXiv:1511.05534 [astro-ph.CO].
- [48] D. H. Lyth and A. R. Liddle, *The Primordial Density Perturbation* (Cambridge University Press, Cambridge, 2009).
- [49] W. Hu and M. J. White, *Phys. Rev. D* **56**, 596 (1997), arXiv:astro-ph/9702170 [astro-ph].
- [50] Available on NERSC, at <http://crd.lbl.gov/departments/computational-science/c3/c3-research/cosmic-microwave-background/cmb-data-at-nersc/>
- [51] Note that a lensing reconstruction will be valid even for the statistical anisotropies considered here.